

Noise induced dimension changing bifurcations

Ira B. Schwartz^a, Lora Billings^b, David S. Morgan^c and Ying Cheng Lai^d

^aNaval Research Laboratory, Plasma Physics Division, Nonlinear Dynamics System Section,
Code 6792, Washington, DC 20375

^bDepartment of Mathematical Sciences, Montclair State University, Montclair, NJ 07043

^cHarvard Medical School - West Quad Computing Group, 240 Longwood Avenue, Boston MA
02115-5701

^dDepartment of Mathematics and Statistics, Department of Electrical Engineering, Arizona
State University, Tempe, AZ 85287

ABSTRACT

The transition to chaos is a fundamental and widely studied problem in deterministic nonlinear dynamics. Well known routes to chaos, which include the period-doubling bifurcation route, the intermittency route, the quasiperiodic route, and the crisis route, describe transitions to low-dimensional chaotic attractors with one positive Lyapunov exponent. Transitions to high-dimensional chaotic attractors with multiple positive Lyapunov exponents have just started being addressed. In stochastic systems, transitions to chaotic-like behavior are less well characterized. Global analysis coupled with stochastic transport probability can explain emergent behavior in which stable and unstable manifolds may interact with noise to cause “stochastic chaos”. Another stochastic route may induce chaotic signatures through a dimension changing bifurcation, whereby the topological dimension changes when the amplitude of the noise goes beyond a critical parameter.

In this paper we present a theory of how the Lyapunov exponents may scale with the noise amplitude in general systems. A physical class of multiscale dynamical systems will be presented to show that noise may induce low dimensional chaos, or for other parameters, may induce chaos that bifurcates to an attractor contained in a high topological dimension. We present a numerical bifurcation analysis of the resulting system, illustrating the mechanism for the onset of high dimensional chaos. By computing the constrained invariant sets, we reveal the transition from low dimensional to high dimensional chaos. Applications include both deterministic and stochastic bifurcations.

1. INTRODUCTION

In many complex spatio-temporal phenomena, both high and low dimensional dynamics may co-exist. Specifically, in systems when there is a spectral splitting of time scales, the dynamics may reside on an inertial manifold which may be quite low dimensional. One field in which this applies is that of coupled structures in continuum mechanics, where slow and fast time scales co-exist, thus exhibiting multi-scale dynamics. Examples of multi-scale behavior have been studied in the flexible spherical pendulum,¹¹ the dynamics of a flexible beam-oscillator system,⁸ and a flexible rod-pendulum system.¹⁰ These examples demonstrate the idea that in addition to a temporal splitting between fast and slow time scales, there also corresponds a geometric splitting. Multi-scale behavior in mechanics is convenient since the model in many instances may be decomposed into a global singular perturbation problem.⁷ Based on a well-developed theory, one may construct rescaled systems for which the dynamics, under suitable hypotheses, may reside on an invariant manifold.⁹

This class of multi-scale engineering structures can have very complicated dynamics. Since the fast part of the problem may be considered an approximation to a perfectly rigid body, it is reasonable to assume that part of the complexity originates within the flexible structure. The geometric splitting yields invariant manifolds which may include chaos within the soft structure.²⁶ On the other hand, for critical parameter choices, the dynamics may leave the manifold, and sample the rest of the phase space, generating a dimension changing bifurcation which includes both fast and slow time scales.²⁶

Although statistical methods are useful for quantifying a dimension change in dynamics, they do not necessarily explain the underlying cause of the bifurcation. In particular, when we think of a dimension bifurcation,

we think of a change in dimension, abrupt or continuous, as a parameter is changed. Normally, the parameter is changed deterministically, resulting in a change in bifurcation structure. This may be explained as sufficiently sampling parts of an attractor off of an invariant manifold. Such bursting is typically observed to be chaotic, which arises from an underlying deterministic chaotic saddle.²² However, another cause of dimension changing chaos may be stochastic. That is, if sufficient noise is added to a low dimensional attractor, it may generate a high dimensional noise induced attractor with a new positive Lyapunov exponent. Noise induced chaos, when produced along with a dimension changing bifurcation, could cause multi-scale behavior in multi-scale systems, such as continuum mechanics. Associated with noise induced chaos is the idea of unstable dimension variability (UDV).

Unstable dimension variability is the changing of the number of local unstable directions along a typical trajectory. Mathematically, it can be described in terms of how a system violates the properties of hyperbolicity. This nonhyperbolicity has been shown to be fundamental to chaotic dynamics, particularly for the problem of shadowing of numerical trajectories in higher dimensions.^{2, 3, 6, 14, 16–18, 25} In Ref. 19, we reported on noise induced chaos in a preliminary mechanics example. There, noise was used to excite a positive Lyapunov exponent. That is, in the absence of a deterministic chaotic attractor, sufficient noise can excite dynamics along unstable manifolds which will accumulate enough statistics to cause a Lyapunov exponent to go positive.

In this paper, we examine scaling laws of dimension changing bifurcations in stochastic mechanical systems. For a complete description of the spatio-temporal deterministic bifurcations, see Ref. 27.

2. NOISE INDUCED CHAOS

In many real systems of interest, noise plays a definitive role with far reaching consequences, in which the qualitative dynamics is changed. For example, in low dimensional noise driven systems, as seen in Refs. 23, 24, and 1, it is possible to induce dynamics which possess a positive Lyapunov exponent. Such a signature is one of the main techniques to measure noise induced chaotic dynamics. In fact, it is possible to generate chaos using additive noise in mechanically driven systems, as seen in the example of driven stochastic mechanics presented in Ref. 19. In this section, we wish to quantify how noise induced chaos is related to a novel mathematical quantity related to the unstable dimensionality of the system. Once the dynamical systems are sufficiently high dimensional, it will be seen how noise interacts with unstable spaces to produce positive Lyapunov exponents. Since flexible continuum mechanical systems produce high dimensional dynamics, the role of noise will be seen to play a prominent role in bifurcation theory.

2.1. Unstable dimension variability and noise-induced chaos

An important phenomenon associated with noise-induced chaos is that unstable dimension variability arises as soon as the attractor becomes chaotic. Unstable dimension variability means that, along a typical trajectory, the number of local unstable directions can change. This is the type of nonhyperbolicity that has been shown to be fundamental to chaotic dynamics, particularly for the problem of shadowing of numerical trajectories in high dimensions.^{2, 3, 6, 14, 16–18, 25} Mathematically, unstable dimension variability can be described in terms of the notion of hyperbolicity (or nonhyperbolicity).

Consider a chaotic set from an N -dimensional map. The set is hyperbolic if the following three conditions are met¹²: (1) At each point in the set the tangent space can be split into an expanding subspace and a contracting subspace. Distances in the expanding (contracting) subspace grow (shrink) exponentially in time; (2) The angle between the stable and the unstable subspaces is bounded away from zero; (3) The expanding subspace evolves into the expanding one along a typical trajectory and the same is true for the contracting subspace. Violation of condition (2) leads to nonhyperbolicity with tangencies, which occurs commonly in low-dimensional chaotic systems with only one unstable direction. Nonhyperbolicity with unstable dimension variability is caused by the violation of condition (3), which occurs in systems with more than one unstable direction, *i.e.*, high-dimensional chaotic systems. In high dimensions, it is common for systems to violate both conditions (2) and (3).

When noise induces a chaotic attractor, unstable dimension variability arises immediately. To see this, consider the situation where there are two coexisting dynamical invariant sets with distinct unstable dimensions. For instance, in the simplest case of a one-dimensional map, in a periodic window an attracting periodic orbit with

zero unstable dimension coexists with a chaotic saddle with unstable dimension one. Another situation, which is quite common, is where there is a periodic attractor and several isolated saddle periodic orbits. The stable and unstable manifolds of these orbits are close to each other and are about to form homoclinic or heteroclinic intersections. The presence of noise can induce dynamics which appear as manifold intersections, creating a chaotic set, the so-called *stochastic chaotic saddle*.^{4,5}

For any periodic point on the attractor, under additive noise of amplitude D a trajectory can be found in a ball of radius D . If D is small so that the ball does not intersect the stable manifold of the chaotic saddle, the final attractor of the system will simply be a fattened version of the original periodic attractor. This is so because a random initial condition leads to a trajectory that is confined in the vicinity of the periodic attractor. Notice, however, there can be transient chaos initially, in the sense that the trajectory may move toward the chaotic saddle along its stable manifold, wander near the saddle for a finite amount of time, and leave it along its unstable manifold. Assume that for $D = D_c$, the noisy ball begins to intersect the stable manifold of the chaotic saddle. For $D > D_c$, there is a nonzero probability that a trajectory in the vicinity of the original periodic attractor is kicked out of the noisy ball and moves toward the chaotic saddle along its stable manifold. Due to the non-attracting nature of the chaotic saddle, the trajectory can stay in its vicinity for only a finite amount of time before leaving along its unstable manifold and then, enter the noisy ball at the original periodic attractor again, and so on. For $D \geq D_c$, the probability for the trajectory to leave the noisy ball of the original periodic attractor is small. Thus, an intermittent behavior can be expected where the trajectory spends long stretches of time near the periodic attractor, with occasional bursts out of it wandering near the chaotic saddle.

A consequence of the noise-induced intermittent behavior is that there is generally unstable dimension variability associated with a continuous trajectory. Under noise, both the chaotic saddle and the original periodic attractor belong to a single, connected dynamical invariant set. Since, in the absence of noise, periodic orbits on the chaotic saddle are all unstable and the attractor is a stable periodic orbit, noise-induced intermittency means that a trajectory moves in regions containing periodic orbits with distinct unstable dimensions. A feature that distinguishes this type of unstable dimension variability with that in the literature^{2,3,6,14,16-18,25} is that here, the subsets with different unstable dimensions are located in distinct regions of the phase space, whereas in high-dimensional chaotic systems found in Refs. 6 and 25, unstable periodic orbits in these subsets tend to mix with each other densely in the phase space.

At a fundamental level, the appearance of unstable dimension variability implies the disappearance of the neutral direction of the flow. Consider a three-dimensional flow in a periodic window, where the periodic attractor contains no unstable direction and the chaotic saddle possesses one unstable dimension. The role of noise, when it is sufficiently large ($D > D_c$), is to link these two dynamical invariant sets with distinct unstable dimensions. Now examine the local eigenplanes that contain the neutral direction of the flow associated with the periodic attractor and the chaotic saddle. In the local eigenplane at the periodic attractor, there is a stable direction and a neutral direction. Consider an eigenvector in the neutral direction. In the eigenplane of a point in the chaotic saddle, there is an unstable direction and a neutral direction. When a trajectory is driven by noise from the periodic attractor to the chaotic saddle along its stable manifold, the eigenvector can lie anywhere in the local eigenplane of the corresponding point in the chaotic saddle. After a time, the vector will be aligned in the unstable direction, due to the expanding dynamics of the chaotic saddle. Distances along the neutral direction of the original periodic attractor can no longer be preserved. This feature of a noisy chaotic attractor is fundamentally different from that of a deterministic chaotic attractor, where a neutral direction always exists. Thus we see that unstable dimension variability plays a fundamental role in shaping the topology of the noisy chaotic flow.

2.2. Scaling law of Lyapunov exponents

Here we sketch an argument that noise-induced chaos implies the largest Lyapunov exponent of the attractor obeys a universal algebraic scaling law:

$$\lambda_1(D) \sim (D - D_c)^\alpha, \text{ for } D \geq D_c, \quad (1)$$

where the scaling exponent α depends on system details. Consider an $(N + 1)$ -dimensional flow in a periodic window. In the absence of noise, the chaotic saddle has K_u positive, one zero, and K_s negative Lyapunov

exponents ($K_u + K_s = N$) which can be ordered as follows:

$$\lambda_{K_u}^{S+} \geq \lambda_{K_u-1}^{S+} \geq \dots \lambda_1^{S+} > 0 = \lambda^{S0} > -\lambda_1^{S-} \geq \dots \geq -\lambda_{K_s-1}^{S-} \geq -\lambda_{K_s}^{S-}. \quad (2)$$

The periodic attractor has one zero and N negative exponents, as follows:

$$0 = \lambda^{P0} > -\lambda_1^{P-} > \dots - \lambda_N^{P-}. \quad (3)$$

For $D < D_c$, an asymptotic trajectory is confined in the neighborhood of the periodic attractor, so the largest Lyapunov exponent of the noisy attractor is simply $\lambda_1 = \lambda^{P0} = 0$. For $D \geq D_c$ (after the transition to chaos), λ_1 is approximately given by

$$\lambda_1 \approx f_P(D)\lambda^{P0} + f_S(D)\lambda_{K_u}^{S+} = f_S(D)\lambda_{K_u}^{S+}, \quad (4)$$

where $f_P(D)$ and $f_S(D)$ are the probabilities that a trajectory stays near the original periodic attractor and the chaotic saddle, respectively. Because of the averaging effect of noise, we expect the dependence on noise of the largest Lyapunov exponent $\lambda_{K_u}^{S+}$ of the original chaotic saddle to be weak. Thus the main dependence of λ_1 on noise comes from $f_S(D)$, the frequency of visit to the chaotic saddle, which is determined by the measure of its stable manifold in the noisy ball of the periodic attractor.

Consider an N -dimensional Poincaré map corresponding to the $(N+1)$ -dimensional flow. For a ball of radius ϵ , the natural measure of the stable manifold contained within is proportional to

$$\epsilon^{d_s} = (\epsilon^N)^{d_s/N},$$

where ϵ^N is proportional to the volume of the ball and d_s is the information dimension of the stable manifold of the chaotic saddle. Using the Kaplan-Yorke conjecture¹⁵ for chaotic saddles,¹³ d_s is given by

$$d_s = K_s + J + \frac{H^S - (\lambda_1^{S+} + \dots + \lambda_J^{S+})}{\lambda_{J+1}^{S+}}, \quad (5)$$

where J is an integer determined by

$$\lambda_1^{S+} + \dots + \lambda_J^{S+} + \lambda_{J+1}^{S+} \geq H^S \geq \lambda_1^{S+} + \dots + \lambda_J^{S+}, \quad (6)$$

and H^S is the forward entropy of the chaotic saddle:

$$H^S = \sum_{i=1}^{K_u} \lambda_i^{S+} - \frac{1}{\tau}. \quad (7)$$

Here τ is the average lifetime of the chaotic saddle on the Poincaré map. (As a practical matter, τ is in the unit of T , the average time that a typical trajectory crosses the Poincaré section.) For $D \geq D_c$, the volume of the noisy ball in which the stable manifold of the chaotic saddle lies is proportional to: $(D^N - D_c^N)$. We thus have

$$\lambda_1 \sim (D^N - D_c^N)^{d_s/N} \sim (D - D_c)^\alpha,$$

which is the scaling law (1) with the algebraic scaling exponent given by

$$\alpha = \frac{1}{N} \left[K_s + J + \frac{H^S - (\lambda_1^{S+} + \dots + \lambda_J^{S+})}{\lambda_{J+1}^{S+}} \right]. \quad (8)$$

Numerical support for the scaling law can be found in Refs. 20 and 19.

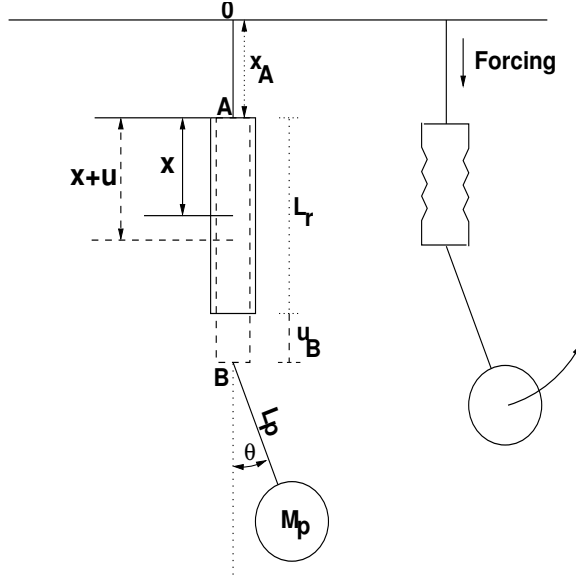


Figure 1. Rod-Pendulum Configuration

3. NOISE INDUCED BIFURCATION AND CHAOS IN MECHANICS

In general, the problems we consider here model linear continua coupled to nonlinear oscillators. That is, the problem class is that of linear PDE's which are coupled to one or more nonlinear oscillators represented by ODE's. Such linear-nonlinear coupled systems are ubiquitous in many applications, and are observed to exhibit nonlinear vibrations in experiments.⁸ In this section, we restrict ourselves to models of linear elastica in one spatial dimension. Such examples include cantilevered beams and extensible rods. In general, if we let $W(\xi, t)$ denote a measure of displacement as a function of space (ξ) and time (t), and let $\varkappa_\mu(\xi, t)$ be a forcing function, then the general equations of motion may be represented as:

$$L_\mu W(\xi, t) = \varkappa_\mu(\xi, t) \quad (9)$$

$$\frac{d^2\theta}{dt^2} + [1 + G(W,_{tt})] \sin \theta + \eta \frac{d\theta}{dt} = 0$$

plus the appropriate boundary conditions. In (9), θ denotes the angular position of an attached pendulum at a free end of the elastica. The term $G(W,_{tt})$ is the additional acceleration imposed on the pendulum from the structure. Since there is an external driving body force on the structure, the function $G(W,_{tt})$ will also contain a time varying source, which will in general depend on another oscillator, such as a mechanical shaker or periodic electric potential.

The differential operator, L_μ , is assumed to be linear, and depends on a parameter which is a measure of spectral splitting of the relevant time scales. For a cantilevered beam, it has the form

$$L_\mu W = \mu^2 \kappa_1^2 W,_{tttt} + W,_{\xi\xi\xi\xi} + 2\zeta_b \mu W,_{t\xi\xi\xi}, \quad (10)$$

while for an extensible rod (detailed below),

$$L_\mu W = \mu^2 W,_{tt} - W,_{\xi\xi} + 2\zeta_r \mu W,_{t\xi\xi}. \quad (11)$$

Normally, the external drive is de-coupled from the rest of the structure. That is, it is assumed that the external drive is one-way coupled to the structure. In this paper, we allow the frequency dependence of the drive to depend weakly on the dynamics of the structure itself.

3.1. Full PDE-ODE system

In formulating the dynamics of such a mutually coupled system, we follow Refs. 22 and 9 in formulating in detail a system of coupled continua. We consider a specific mechanical system consisting of a vertically positioned viscoelastic linear rod of density ρ_r , with cross-section A_r and length L_r , with a pendulum of mass M_p and arm length L_p coupled at the bottom of the rod and where the rod is forced from the top harmonically with frequency Ω and magnitude α .⁹ The rod obeys the Kelvin-Voigt stress-strain relation²¹ and E_r and C_r denote the modulus of elasticity and the viscosity coefficient. C_p is the coefficient of viscosity (per unit length) of the pendulum and g is the gravitational constant of acceleration. The pendulum is restricted to a plane, and rotational motion is possible. The system is modeled by the by coupling a PDE modeling the displacement to an ODE system modeling an oscillator²⁷:

$$\begin{aligned} M_p L_p \ddot{\theta} + M_p [g - \ddot{x}_A - \ddot{u}_B] \sin(\theta) + C_p L_p \dot{\theta} &= 0 \\ A_r \rho_r \ddot{u}(x, t) - A_r E_r u''(x, t) - A_r C_r \dot{u}''(x, t) - A_r \rho_r (g - \ddot{x}_A) &= 0, \end{aligned} \quad (12)$$

where $\dot{} \equiv \frac{\partial}{\partial t}$, and $' \equiv \frac{\partial}{\partial x}$, with boundary conditions

$$u(x=0, t) = 0, \quad A_r E_r \left. \frac{\partial u}{\partial x} \right|_{x=L_r} = A_r E_r \frac{\partial u_B}{\partial x} = T_p \cos(\theta),$$

and where

$$T_p = M_p L_p \dot{\theta}^2 + M_p (g - \ddot{x}_A - \ddot{u}_B) \cos(\theta)$$

denotes the tension acting along the rigid arm of the pendulum. The variable $u(x, t)$ denotes the displacement field of the uncoupled rod with respect to the undeformed configuration at equilibrium, relative to the point A , while u_B denotes the relative position of the coupling end B of the rod with respect to point A . See Fig. 1 for a schematic of the rod and pendulum system.

We further suppose that the drive at A , given by the function $x_A(t)$ in (12), is such that it comes from another oscillator. We suppose that the oscillator is weakly coupled to the pendulum through its frequency. Specifically, we model the drive oscillator by

$$\begin{aligned} \dot{\Phi}_1 &= \Phi_1 + \Omega(1 + \Sigma P(\dot{u}(x, t)))\Phi_2 - \Phi_1(\Phi_1^2 + \Phi_2^2) \equiv F_1(\Phi_1, \Phi_2, \Sigma, \Omega) \\ \dot{\Phi}_2 &= -\Omega(1 + \Sigma P(\dot{u}(x, t)))\Phi_1 + \Phi_2 - \Phi_2(\Phi_1^2 + \Phi_2^2) \equiv F_2(\Phi_1, \Phi_2, \Sigma, \Omega), \end{aligned} \quad (13)$$

where P is a projection onto a Fourier mode (see below), and $|\Sigma| \ll 1$ is the coupling term that modulates the frequency. Notice that when $\Sigma = 0$, the solution of (13) consists of sines and cosines of frequency ω given the appropriate initial conditions. In terms of the solutions to (13), note that $x_A(t) = \Phi_2(t, \Sigma)$.

Equations 12 and 13 are nondimensionalized by the following variable re-scalings

$$\begin{aligned} \xi &= \frac{x}{L_r}, \quad \tau = \omega_p t, \\ X_A &= \frac{x_A}{L_p}, \quad U = \frac{u}{L_p}, \quad U_B = \frac{u_B}{L_p}, \end{aligned}$$

and parameter re-scalings

$$\begin{aligned} \mu &= \frac{\omega_p}{\omega_1}, \quad \mu_m = \frac{\omega_1}{\omega_m} = \frac{1}{2m-1}, \quad \beta = \frac{M_p}{A_r \rho_r L_r} \\ \zeta_p &= \frac{1}{2\omega_p} \frac{C_p}{M_p}, \quad \zeta_r = \frac{1}{2\omega_1} \frac{\pi^2 C_r}{4L_r^2 \rho_r}, \end{aligned}$$

where

$$\omega_p = \sqrt{\frac{g}{L_p}}, \quad \omega_m = \frac{\pi(2m-1)}{L_r} \sqrt{\frac{E_r}{\rho_r}}, \quad m = 1, 2, \dots, \infty,$$

are the natural frequency of the uncoupled pendulum and the spectrum of natural frequencies of the uncoupled flexible rod, respectively, while ζ_p and ζ_r denote their damping factors.

Using the parameter re-scalings, and setting time derivatives equal to zero, the stable and unstable static equilibrium configurations of the coupled rod and pendulum system are given by (θ_c, \hat{U}) and $(\theta_{S\pm}, \hat{U})$, where

$$\begin{aligned}\theta_c &= 0, & \theta_{S\pm} &= \pm\pi \\ \hat{U} &= \frac{\mu^2\pi^2}{2} [2(1+\beta)\xi - \xi^2].\end{aligned}$$

The normalized equations are thus

$$\begin{aligned}\ddot{\theta} + [1 - \ddot{V}_B(\tau) - \ddot{X}_A(\tau)] \sin(\theta) + 2\zeta_p\dot{\theta} &= 0, \\ \mu^2\pi^2\ddot{V}(\xi, \tau) - V''(\xi, \tau) - 8\zeta_r\mu\dot{V}'''(\xi, \tau) &= -\mu^2\pi^2\ddot{X}_A(\tau) \\ V(\xi=0, \tau) = 0, & \quad V'(\xi=1, \tau) = -\mu^2\beta\pi^2[1 - T\cos(\theta)],\end{aligned}\tag{14}$$

where

$$V(\xi, \tau) = U(\xi, \tau) - \hat{U}(\xi), \quad 0 \leq \xi \leq 1, \quad -\infty < \tau < +\infty,$$

and note that we redefine $\dot{\cdot} \equiv \frac{\partial}{\partial\tau}$ and $' \equiv \frac{\partial}{\partial\xi}$ for the remainder of the paper.

3.2. Projection onto a finite modal

In carrying out our analysis, we will consider a reduction of the ODE/PDE system in (14). This reduction is obtained by performing a modal expansion of the rod equation, where the displacement V is expanded as $V(\xi, \tau) = \sum_{m=1}^{\infty} \eta_m(\tau)\phi_m(\xi)$. This results in an infinite system of coupled oscillators,

$$\begin{aligned}\ddot{\theta} &= - \left[1 + \sum_{j=1}^{\infty} (-1)^{j+1} \dot{\eta}_j - \ddot{X}_A(\tau) \right] \sin(\theta) - 2\zeta_p\dot{\theta} \\ L_m(\theta)\ddot{\eta}_j &= - \frac{\eta_m}{4\eta^2\eta_m^2} + 2\zeta_r \frac{\dot{\eta}_m}{\mu\mu_m^2} - (-1)^{m+1}2\beta \left[\dot{\theta}^2 \cos(\theta) - \sin^2(\theta) \right] \\ &\quad - \left[\frac{4\mu_m}{\pi} + (-1)^{m+1}2\beta \cos^2(\theta) \right] \ddot{X}_A(\tau),\end{aligned}\tag{15}$$

equivalent to (12), where $L_m(\theta)$ is the infinite linear operator

$$L_m(\theta) \equiv \sum_{j=1}^{\infty} [\delta_{mj} + (-1)^{m+j}2\beta \cos^2(\theta)].$$

See Ref. 22 for the details of this transformation.

The primary parameter governing the coupling between the rod and pendulum is the ratio of the natural frequency of the pendulum to the frequency of the first rod mode, $\mu \equiv \omega_p/\omega_1$. In the limit $\omega_1 \rightarrow \infty$, the rod is perfectly rigid, $\mu \rightarrow 0$, and the system reduces to a forced and damped pendulum. For $0 < \mu \ll 1$ sufficiently small, global singular perturbation theory predicts that system motion is constrained to a slow manifold, and the (fast) linear rod-modes are slaved to the slow pendulum motion.⁷ For nonzero α (the amplitude of the periodic forcing) the slow manifold is a non-stationary (periodically oscillating) two-dimensional surface.

For our study, we set the number of modes in the structure to be unity, and consider the following reduced

system:

$$\begin{aligned}
\dot{\Psi}_1 &= \Psi_2 \\
\dot{\Psi}_2 &= (\pi\Psi_2(-2\zeta_p - 4\beta\zeta_p \cos^2(\Psi_1) + \beta \sin(2\Psi_1)\Psi_2) - \sin(\Psi_1)(4\alpha\Psi_4 \\
&\quad + 4\alpha\beta\pi \cos^2(\Psi_1)\Psi_4 + \pi(1 + 2\beta + Z_1 + 2\zeta_r Z_2 + \alpha\Psi_4)))/(\pi\delta) \\
\dot{\Psi}_3 &= \Psi_3(1 - (\Psi_3^2 + \Psi_4^2)) + \Omega(1 + \sigma\Psi_2)\Psi_4 \\
\dot{\Psi}_4 &= \Psi_4(1 - (\Psi_3^2 + \Psi_4^2)) - \Omega(1 + \sigma\Psi_2)\Psi_3 \\
\dot{Z}_1 &= Z_2/\mu \\
\dot{Z}_2 &= -(2\beta\pi - 2\beta\pi \cos(\Psi_1)\Psi_2^2 + \pi Z_1 + 2\pi\zeta_r Z_2 + 4\alpha\Psi_4 \\
&\quad + 2\beta\pi \cos^2(\Psi_1)(-1 + \alpha\Psi_4))/(\mu\pi\delta)
\end{aligned} \tag{16}$$

where $\delta = 1 + 2\beta \cos(\Psi_1)$. In (16), Ψ_1 and Ψ_2 are the pendulum position and velocity, Ψ_3 and Ψ_4 are the drive oscillator variables, and Z_1 and Z_2 are the rod mode position and velocity. Notice that the singular perturbation parameter denotes the rod variables to have a fast time scale compared to the pendulum and drive. Also, the frequency of the drive oscillator is a function of the pendulum momentum, which is a feedback term. The system in (16) is therefore fully coupled, which is a generalization of the more ideal case of having a perfectly isolated drive.

We study the transition to stochastic chaos when we add stochastic perturbations of the form

$$\frac{dy}{dt} = \mathbf{F}(\mathbf{y}, p) + D\xi(t)$$

where \mathbf{F} is the deterministic vector field of the mechanical system defined in (16), p represents the vector of parameters, and $D\xi(t)$ is the additive Gaussian white noise with standard deviation D . Note that $\xi(t)$ is an 6-dimensional vector whose components are independent Gaussian random variables of zero mean and scaled variance. Explicitly, the noise is scaled in each component so that it does not dominate components with smaller magnitudes. We find the approximate range of each variable when it is in its steady state and then scale the standard deviation of the noise by those factors so that it effects each component equally. Noise is not added to the components representing the drive (Ψ_3 and Ψ_4 in (16)), so those variances are set to zero. We also integrate the Jacobian and calculate the Floquet multipliers to find the Lyapunov exponents based on time averaging. By fixing the parameters of (16), we examine the dynamics of the mechanical random dynamical system as the noise amplitude is increased from zero.

First, we study the system with small coupling using the parameters $\mu = 0.086875$ and $\alpha = 1.8$. With no noise, the dominant behavior of the system is a chaotic attractor on the slow manifold characterized by one positive Lyapunov exponent. As expected with an autonomous flow, the second largest exponent is the null Lyapunov exponent, which represents the neutral direction associated with the flow. The four remaining Lyapunov exponents are negative. Adding noise to the system excites a nearby high dimensional chaotic saddle off the slow manifold and the potential number of unstable (dynamical) dimensions is increased from one to two. Numerically, we observe that increasing the standard deviation of the noise (D) increases the third Lyapunov exponent, the largest negative exponent, in a continuous manner. When the third exponent is close to crossing zero, the null exponent increases away from zero, leaving no zero valued Lyapunov exponent within a small window. Define the beginning of this transition D_c . This fundamentally disturbs the noisy flow, resulting in two positive Lyapunov exponents and the third largest exponent approaching the zero value from the negative side. See Fig. 2a for a graph of this transition. We approximate the algebraic scaling of the Lyapunov exponent with a least squares fit as $a = 1.5143$, having a maximum error of 0.5786, as shown in Fig. 2b.

At larger coupling parameters, the dominant behavior of the system is a periodic attractor. Therefore, with no noise, all the Lyapunov exponents are negative except for the null exponent. The addition of noise emulates chaotic behavior, which is observed by the bifurcation in the Lyapunov exponents from zero to two local unstable directions. We use the parameters $\mu = 0.5025$ and $\alpha = 0.65$ as an example in Fig. 3. Notice that the two largest exponents increase in a continuous manner above zero and the third largest approaches zero from the negative side in Fig. 4a. This is a new type of transition to noise induced chaos. The largest Lyapunov exponent follows

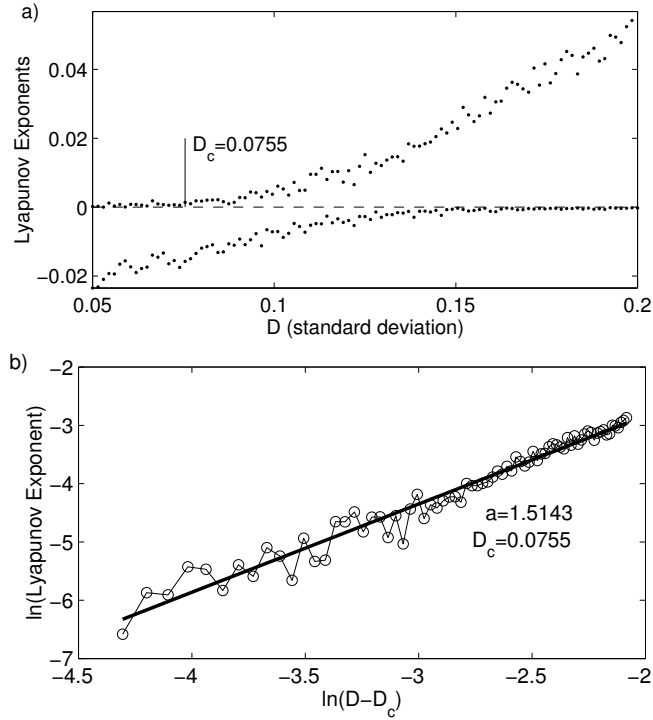


Figure 2. For the noisy system in the small coupling case, (a) the second and third Lyapunov exponents versus D about the transition, and (b) algebraic scaling of the second largest Lyapunov exponent with $D - D_c$. The solid line in indicates the theoretical slope a .

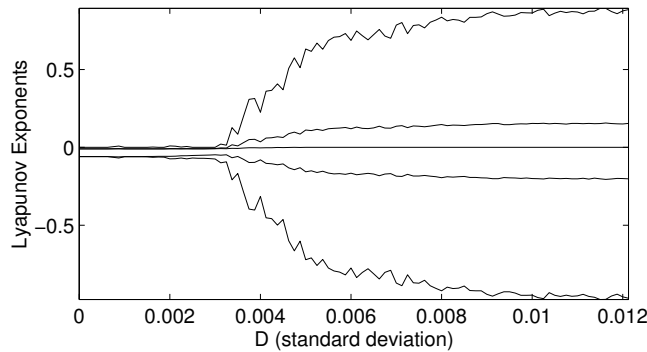


Figure 3. The Lyapunov exponents of the noisy system. This is the large coupling case using the parameters $\mu = 0.5025$ and $\alpha = 0.65$.

an algebraic scaling similar to the one shown in the small coupling case. We use $D_c = 0.002938$, which results in a linear fit with slope 1.4973 and maximum error of 0.8087. The second largest exponent also follows an algebraic scaling, but it increases from a negative value. Therefore, we must translate the Lyapunov exponent by that negative value so we can use the natural log. We use the value of the Lyapunov exponent at D_c , called L_c , and find $\ln(L - L_c)$ as we increase D from D_c . This results in a linear fit with slope 1.5090 and maximum error of 0.8198. Note the similarity in this scaling to that of the maximum Lyapunov exponent. Graphs of each of these fits are shown in Fig. 4b. Because this example uses a large coupling parameter, the dynamics are not dominated by the slow manifold and we cannot compute bursting statistics similar to the previous example.

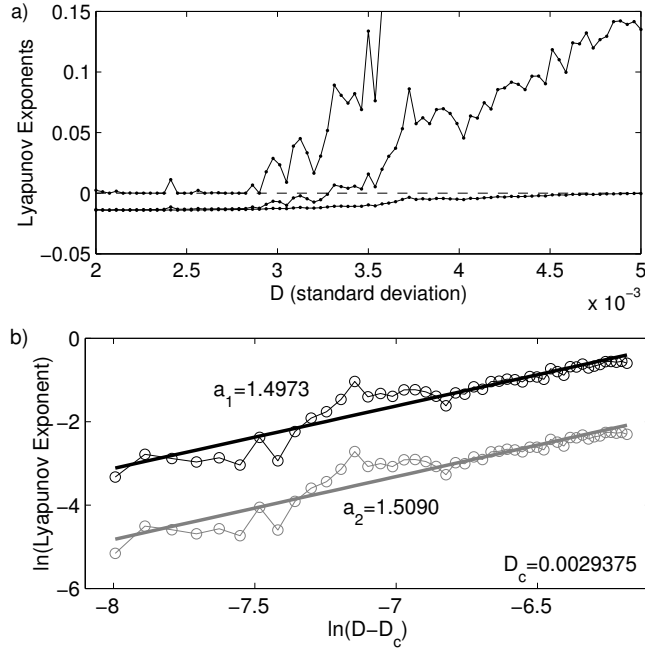


Figure 4. These graphs use the noisy system with large coupling parameters: $\mu = 0.5025$ and $\alpha = 0.65$. a) A close up of the three largest Lyapunov exponents near the transition to stochastic chaos. b) The algebraic scaling for the two largest Lyapunov exponents. The largest exponent is shown in black and the data is plotted $\ln(L)$ vs. $\ln(D - D_c)$. The second largest is in grey and the data is plotted $\ln(L - L_c)$ vs. $\ln(D - D_c)$. Both linear fits have slope close to 1.5.

4. CONCLUSIONS

One important aspect of the noise induced bifurcation was quantifying the relationship of the change in Lyapunov exponents with respect to the standard deviation of the noise. We sketched an argument to show how UDV in stochastic systems results in a universal scaling law in the top Lyapunov exponents. Here we used the unstable dimension variability of the system to show explicitly in a multi-scale system that the exponent obeys a universal scaling law. It is a remarkable fact that the scaling actually persists over a wide range of noise amplitudes. It is also an interesting observation that the change is continuous, even when the deterministic changes from periodic to hyper-chaotic behavior are discontinuous.

Acknowledgments

IBS is supported by the Office of Naval Research. DSM is currently an NRC post doctoral fellow. YCL is supported by AFOSR under Grant No. F49620-03-1-0290. LB is supported by the NSF under Grants DMS-0414087 and CTS-0319555.

REFERENCES

1. L. Arnold, N. S. Namachchivaya, and K. R. SchenkHoppe. Toward an understanding of stochastic hopf bifurcation: A case study. *International Journal Of Bifurcation And Chaos*, 6:1947–1975, 1996.
2. E. Barreto and P. So. Mechanisms for the development of unstable dimension variability and the breakdown of shadowing in coupled chaotic systems. *Phys. Rev. Lett.*, 85:2490–2493, 2000.
3. E. Barreto, P. So, B. J. Gluckman, and S. J. Schiff. From generalized synchrony to topological decoherence: emergent sets in coupled chaotic systems. *Phys. Rev. Lett.*, 84:1689–1692, 2000.
4. L. Billings, E. M. Bollt, and I. B. Schwartz. Phase-space transport of stochastic chaos in population dynamics of virus spread. *Phys. Rev. Lett.*, 88:234101, 2002.

5. L. Billings and I. B. Schwartz. Exciting chaos with noise: unexpected dynamics in epidemic outbreaks. *J. Math. Biol.*, 44:31–48, 2002.
6. S. P. Dawson, C. Grebogi, T. Sauer, and J. A. Yorke. Obstructions to shadowing when a lyapunov exponent fluctuates about zero. *Phys. Rev. Lett.*, 73:1927–1930, 1994.
7. N. Fenichel. *J. Diff. Eq.*, 53, 1979.
8. I. T. Georgiou, I. Schwartz, E. Emaci, and A. Vakakis. Interaction between slow and fast oscillations in an infinite degree-of-freedom linear system coupled to a nonlinear subsystem: Theory and experiment. *Journal Of Applied Mechanics-Transactions Of The Asme*, 66:448–459, 1999.
9. I. T. Georgiou and I. B. Schwartz. Dynamics of large scale coupled structural mechanical systems: A singular perturbation proper orthogonal decomposition approach. *Siam Journal On Applied Mathematics*, 59:1178–1207, 1999.
10. I. T. Georgiou and I. B. Schwartz. The non-linear slow normal mode and stochasticity in the dynamics of a conservative flexible rod/pendulum configuration. *Journal Of Sound And Vibration*, 220:383–411, 1999.
11. I. T. Georgiou and I. B. Schwartz. Invariant manifolds, nonclassical normal modes, and proper orthogonal modes in the dynamics of the flexible spherical pendulum. *Nonlinear Dynamics*, 25:3–31, 2001.
12. J. Guckenheimer and P. Holmes. *Nonlinear Oscillations, Dynamical Systems, and Bifurcations of Vector Fields*. Springer-Verlag, New York, 1983.
13. B. R. Hunt, E. Ott, and J. A. Yorke. Fractal dimensions of chaotic saddles of dynamical systems. *Phys. Rev. E.*, 54:4819–4823, 1996.
14. H. Kantz, C. Grebogi, A. Prasad, Y.-C. Lai, and E. Sinde. Unexpected robustness of a class of nonhyperbolic chaotic attractors against noise. *Phys. Rev. E.*, 65:026209, 2002.
15. J. L. Kaplan and J. A. Yorke. Chaotic behavior of multidimensional difference equations. In H. O. Peitgen and H. O. Walter, editors, *Lecture Notes in Mathematics*, volume 730. Springer, Berlin, 1979.
16. E. J. Kostelich, I. Kan, C. Grebogi, E. Ott, and J. A. Yorke. Unstable dimension variability: A source of nonhyperbolicity in chaotic systems. *Physica D*, 109:81–90, 1997.
17. Y.-C. Lai and C. Grebogi. Modeling of coupled chaotic oscillators. *Phys. Rev. Lett.*, 82:4803–4806, 1999.
18. Y.-C. Lai, D. Lerner, K. Williams, and C. Grebogi. Unstable dimension variability in coupled chaotic oscillators. *Phys. Rev. E*, 60:5445–5454, 1999.
19. Y.-C. Lai, Z. Liu, L. Billings, and I. B. Schwartz. Noise-induced unstable dimension variability and transition to chaos in random dynamical systems. *Phys. Rev. E*, 67:026210, 2003.
20. Z. Liu, Y.-C. Lai, L. Billings, and I. B. Schwartz. Transition to chaos in continuous-time random dynamical systems. *Phys. Rev. Lett.*, 88:124101, 2002.
21. L.E. Marven. *Introduction to the Mechanics of a Continuous Medium*. Prentice-Hall, Englewood Cliffs, 1969.
22. Davis M. Morgan, Erik Bollt, and Ira B. Schwartz. Constructing invariant sets in multi-scale continuum systems. *Physical Review E*, in press, 2003.
23. N. S. Namachchivaya and N. Ramakrishnan. Stochastic dynamics of parametrically excited two d.o.f. systems with symmetry. *Journal Of Sound And Vibration*, 262:613–631, 2003.
24. N. S. Namachchivaya and H. J. Van Roessel. Moment lyapunov exponent and stochastic stability of two coupled oscillators driven by real noise. *Journal Of Applied Mechanics-Transactions Of The Asme*, 68:903–914, 2001.
25. T. Sauer, C. Grebogi, and J. A. Yorke. How long do numerical chaotic solutions remain valid? *Phys. Rev. Lett.*, 79:59–62, 1997.
26. I. B. Schwartz and I. T. Georgiou. Instant chaos and hysteresis in coupled linear-nonlinear oscillators. *Physics Letters A*, 242:307–312, 1998.
27. I. B. Schwartz, D. S. Morgan, L. Billings, and Y.-C. Lai. Multi-scale continuum mechanics: From global bifurcations to noise induced high dimensional chaos. *CHAOS*, 14:373–386, 2004.